Vortex-Shedding-Induced Dissipation of Waves Scattering against Surface-Piercing Vertical Thin Plates
수면에 거치된 수직 다중 판에 의한 산란에서 와류로 인한 파랑 에너지의 소멸

Mi Ran Oh[1] and Jung Lyul Lee[1]
오미란[1] · 이정렬[1]

1. Introduction

The breakwater of surface-piercing type has been developed mainly for application within bays or estuaries that are semi-protected from the direct impact of large waves. Most of bays have soft foundation which is too weak to bear the weight of gravity type breakwater. Thus the surface-piercing barrier is taken into account as an alternative tool to reduce wave heights in the bay to an acceptable level. Differently from the ordinary breakwater of gravity type, the surface barrier reduces the transmitted waves mainly due to the reflection of incident waves from the barrier body. Traditional breakwaters, seawalls and jetties reflect or direct wave energy in destructive ways or concentrate it in local hot spots so that the concentrated energy leads to the destruction of marine facilities. Among a number of breakwaters, the vertical barriers with gaps are recently favored from the point of view of marine environment since they do not in general partition the natural sea. Free exchange of water mass through the structures is possible so that the water in the sheltered region can be kept circulating and therefore prevent stagnation and pollution.

The scattering of water waves by such structures has been solved previously by a number of authors but well known for the mathematical difficulties encountered within the framework of linearized potential theory. Therefore, vertical barrier performance by theoretical evaluations has been typically accomplished in the two-dimensional domain, in which the wave transmission and reflection characteristics are only taken into account. In harbors and marinas, however, incoming waves may be significantly diffracted and radiated beyond such structures and consequently reflected by harbor warves and returned to them. Under such circumstances, it is essential for the wave-induced motion in a harbor to be solved numerically with taking into account the effect of wave deformation in a harbor.

The numerical approaches of the wave-structure interaction have concerned several authors. Sawaragi et al. (1987) proposed a numerical method combining a three-dimensional Green's function model for near-field waves around a floating body and a two-dimensional BIEM model for far-field waves. Recently, Ohyama and Tsuchida (1997) expanded the mild-slope equation incorporating evanescent modes to get much higher computational efficiency as compared to previous approaches. However, their new sets of mild-slope equations for evanescent modes still require significant CPU time and computational storage. As more simple approach for vertical barriers, Lee and Lee (2001) and Lee and Lee (2003) proposed a plane wave method to add scattering terms to the traditional mild-slope

---

1 성균관대학교 토목환경공학과 (Corresponding Author : Mi Ran Oh, Department of Civil and Environmental Engineering, Sungkyunkwan University, Chunchun-Dong, Jangan-Ku, Suwon, 440-746, Korea, namu387@skku.edu)

equation without inclusion of evanescent modes. The scattering term, which generates the scattering waves, is determined by the gradient of surface velocity potential across the barrier. Evanescent modes are only considered in predicting the reflection ratio against the vertical barrier.

In this study, an extension is made to allow for some arbitrary dissipation of energy associated with the interaction of waves with each barrier. The present approach is applied to analyze the combined effects of energy dissipation due to vortex shedding from the lower edges of a number of vertical barriers of arbitrary configuration. We use Stiassnie (1984)'s formula describing the energy dissipation coefficient due to a vortex motion in a single barrier.

Model performance is examined for a scattering problem where the local evanescent modes are ignored. The numerical results are compared with experimental data carried out in the wave flume.

2. Mild-Slope Equation

2.1 Governing equation

We derive a set of MSE starting from the time-dependent MSE proposed by Smith and Sprinks (1975) as follows:

$$\frac{\partial^2 \eta}{\partial t^2} - \nabla \left(CC_g \nabla \eta \right) + (\sigma^2 - k^2 CC_g)\eta = 0 \quad (1)$$

where, η is the free surface displacement, C the wave celerity, C_g the group velocity. From the dynamic free surface boundary, $\nabla \eta$ can be expressed by velocity vector, **u** defined at the free surface as follows:

$$\nabla \eta = -\frac{1}{g} \frac{\partial u}{\partial t} \quad (2)$$

where g is the gravitational acceleration. Therefore, Eq. (1) becomes

$$\frac{\partial^2 \eta}{\partial t^2} + \nabla \cdot \left(CC_g \frac{1}{g} \frac{\partial u}{\partial t} \right) + (\sigma^2 - k^2 CC_g)\eta = 0 \quad (3)$$

The above equation is combined with

$$\frac{\partial u}{\partial t} + g\nabla \eta = 0 \quad (4)$$

It is noticeable that Eqs. (3) and (4) allow the wave energy propagating with a group velocity differently from the set of Copeland (1985)'s wave equations. Similarly as done by Madsen and Larsen (1987) for regular waves, the above equations are reformulated by extracting the harmonic time variation with letting $\eta = Sexp(-i\sigma t)$ and $u = Uexp(-i\sigma t)$ so as to speed up the solution considerably since one does not need to resolve the wave period any longer.

$$\frac{\partial^2 S}{\partial t^2} - 2i\sigma \frac{\partial S}{\partial t} + \nabla \cdot \left[\frac{CC_g}{g} \left(\frac{\partial U}{\partial t} + i\sigma U \right) \right]$$
$$- k^2 CC_g S = S_i \quad (5a)$$

$$\frac{\partial U}{\partial t} - i\sigma U + g\nabla S = U_s \quad (5b)$$

where S_i is the source term which generates the incoming waves and U_s is the scattering term defined in the next subsection. The source term is given in terms of the incident wave height H_i on the grid mesh of Δx and Δy:

$$S_i = \sigma C_g H_i exp(ik \, sin\theta_i y)\frac{\Delta s}{\Delta x \Delta y} \quad (6)$$

where θ_i is the incident wave direction, and Δs is the width of the incident wave front inside a mesh. A new set of combined differential equations (5a) and (5b) as shown above can be applied in most effective engineering practice to assess the irregular wave conditions as well as regular in existing or proposed new harbors.

2.2. Scattering term

A thin barrier can be taken into account as another source of wave generating because it generates scattering waves. As shown in Eq. (5a), the scattering term is given in the momentum equation since it is expressed in terms of U which is continuous across a barrier. The scattering term can be determined as the added volume of water divided by the area of the grid mesh and time step. To generate U which corresponds to R_v inside the model boundaries, the term is given by

$$U_s = 2C\frac{\Delta s}{\Delta x \Delta y}R_v \qquad (8)$$

where Δs is the width of the barrier inside a mesh (see Madsen and Larsen, 1987). The added amount will propagate in two opposite directions from the barrier. Since R_v is given by Ur/t, Eq. (8) is now expressed in terms of τ as

$$U_s = 2C\frac{r}{t}\frac{\Delta s}{\Delta x \Delta y}U \qquad (9)$$

For the case of energy conservation [see Mei (1983)],

$$\frac{r}{t} = \pm\,i\,\frac{|r|}{|t|}$$

Thus the conventional mild-slop equation was modified with an additional term inserted. Note that this equation is computationally effective as well as applicable for scattering on the varying depth.

2.3. Numerical scheme

The governing equations are solved by the approximate factorization techniques leading to the implicit finite difference schemes. The scheme is applied with the complex variables defined on a space-staggered rectangular grid. Since the matrix coefficients of the corresponding difference equations form a tridiagonal matrix, they are solved by using the tridiagonal algorithm which is widely used in solving finite difference equations because of its great efficiency. The more detailed description such as the treatment of side boundary condition and partial as well as free reflecting wall condition is given in Lee (1998).

3. Energy Dissipation due to Vortex Shedding

In nature, the presence of the obstacle may induce vortex breakdown, which in turn introduces vorticity in the flow. The most important consequence of vorticity production is energy dissipation at the expense of the transmitted waves. So now we consider the waves whose energy is dissipated.

Energy losses due to vortex shedding from the lower edge of a vertical plate attacked by surface waves. The energy dissipation coefficient, which is determined as the ratio between the flux of the energy taken out by the vortex generation process, and the incoming wave energy flux, is given by (Stiassnie at al., 1984) as

$$e \sim \frac{2.16\,(ka_o)^{(2/3)}}{ka\,[K_1^2\,(ka) + \pi I_1^2\,(ka)]^2} \qquad (10)$$

where, a_o and k are the amplitude and wave number of the incoming wave, respectively, and a is the draught of the plate. This theoretically derived formula, which is only valid for infinitely deep water, appeared to be in good agreement with experimental data but The formula given in Eq. (10) should be modified so that the coefficient is less than 1 in all frequencies.

For the energy dissipation coefficient, e, we get in terms of reflection and transmission coefficients as

$$r_- t_+^* + r_+^* t_- = e \qquad (11)$$

where $()^*$ denotes the complex conjugate. Multiply Eq. (11) by $t_+ r_+$ yields

$$|t_+|^2 r_- r_+ + |r_+|^2 t_- t_+ = e t_+ r_+ \qquad (12)$$

and dividing Eq. (12) by $t_- t_+$,

$$|t_+|^2 \frac{r_- r_+}{t_- t_+} - e\frac{r_+}{t_-} + |r_+|^2 = 0 \qquad (13)$$

where $t_- = t_+ = t$.

In the case of a symmetric body, $r_- = r_+ = r$. Thus Eq. (13) becomes

$$|t_+|^2 \frac{r^2}{t^2} - e\frac{r}{t} + |r_+|^2 = 0 \qquad (14)$$

which yields the solutions

$$\alpha = \frac{r}{t} = \frac{e/2 \pm \sqrt{e^2/4 - |r|^2|t|^2}}{|t|^2} \qquad (15)$$

In the special case of no dissipation, Eq. (15) becomes

$$\alpha = \frac{r}{t} = \pm\, i\,\frac{|r|}{|t|} \qquad (16)$$

as given by (Mei, 1986). Hereafter the minus sign is taken of $\pm$ signs after a comparison with the well-known single-barrier solutions of Ursell (1947).

We rewrite Eq. (16) in terms of r_o and t_o, which are determined under no dissipation. We introduce a new factor, ϵ, as the assignment factor of dissipating energy, which is empirically determined. Then, the relations between $|r|$ and $|r_o|$ and between $|t|$ and $|t_o|$, respectively, to satisfy $|r|^2+|t|^2+e=|r_o|^2+|t_o|^2=1$ can be given as follows:

$$|r|^2 = |r_o|^2 + \epsilon - e/2, \quad |t|^2 = |t|^2 - \epsilon - e/2 \qquad (17)$$

Thus $\epsilon=0$ implies that the energy dissipation equally assigned to reflection and transmission coefficients, while $\epsilon=e/2$ implies that all energy dissipation occurs when waves transmit. Figure 1 presented by Stiassnie at al. (1984) shows that the energy losses due to the vortex shedding from the lower edge of a vertical plate occurs when waves transmit.

Fig. 1. Reflection and transmission coefficients for vertical thin plate. Full symbols are for transmission; hollow symbols are for reflection; the crosses are for energy dissipation (from Stiassnie at al., 1984).

Substituting Eq. (17) into Eq. (16) gives

$$\alpha = \frac{r}{t} = \frac{e/2 - i\,\sqrt{(|r_o|^2 + \epsilon)(|t_o|^2 - \epsilon) - e/2}}{|t_o|^2 - \epsilon - e/2} \qquad (18)$$

Energy losses due to vortex-shedding can be embodied by applying Eq. (10) to Eq. (18), and Eq. (18) is applied to Eq. (9).

4. Performance Test

Figure 2 shows the model performance of wave reflection and transmission for energy dissipation calculated by Eq. (10). The model was run for two amplitudes of 5 and 10cm, respectively, to examine the effect of wave amplitudes. Because of use of $\epsilon=e/2$, there is no change in both the theoretical and numerical results for the reflection coefficient in the figure while the transmission decreases with increasing wave amplitudes. Thus it implies that the scattering waves are generated well by the scattering term given in Eq. (9) which is applied to MSE as shown in Eq. (5).
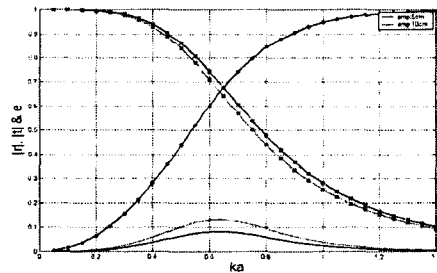

Fig. 2. Performance test of wave reflection and transmission from a vertical barrier (lines: given values, symbols: model results).

Now we compare the model results for a surface barrier shown in Fig. 3a with Ursell's solutions (Ursell, 1947), which are expressed by Bessel functions as solutions valid for deep-water waves. In Fig. 3b, variation of normalized wave heights divided by an incident wave height, H/H_0, are shown against normalized distance divided by the wave length L, x/L. The model calculation was performed on the mesh of the number of grid of 201 and grid size of 0.199m using the wave number $k=1m^{-1}$ and $a=1m$. The barrier is located at $x=0$ which is the center of computational domain. It shows that deviation from the Ursell's solutions

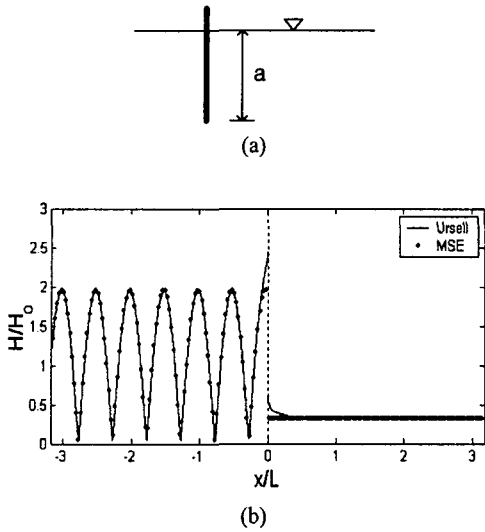decreases with getting away from the barrier. However, they are indistinguishable for $x > L/4$.

(a)

(b)

Fig. 3. Comparison with Ursell's solution for a vertical barrier located at $x = 0$ a) sketch of surface barrier, b) variation of wave heights for $k=1/m$ and $a=1m$.

5. Physical Experiments

The surface-piercing breakwater was set in a Sungkyunkwan University wave flume consisted of a wave generator and a harbor with surface-piercing breakwater model as shown in Fig. 4.

The flume is $12m$ long, $0.4m$ wide and $0.5m$ deep with the still water depth being maintained at $0.2m$. The whole length of a harbor is $1.5m$. the end of harbor is closed by an impermeable wall and the spacing of barrier is $0.462m$ as shown in Fig. 4. The regular waves were generated by the piston-type wave paddle. The bottom and sides walls of the flume are glass to allow easy optical access. At the other end of the flume, there is an absorbing beach zone to disperse the remaining wave energy and to limits reflections.

As shown in Fig. 5, the wave flume was decorated with the data acquisition system accessing the wave profile signals from the gages. Gages were connected with an amplifier. Then the DaqBoard 100A (DaqBoard), A/D converter, changes conditioned signals into corresponding digital numbers saved as ASCII format.
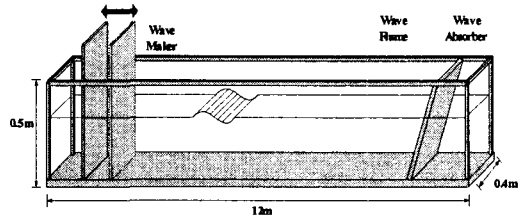

Fig. 4. Wave flume, generator and absorber.

Physical experiments were accomplished for two different wave periods as given in Table 1. The incident wave heights were measured without a harbor model. We assume that the reflective waves against a harbor model are ignorable because the harbor width of $8cm$ is relatively narrow when compared with the flume width of $40cm$. The layout of experimental configuration is illustrated in Fig. 5, showing the locations of the measurement stations and detailed geometry of the flume. The model calculation was performed on the grid mesh of 290×52 and grid size of $8mm$. Figs. 6 and 7 show the comparison between the numerical results and measured wave profiles. With inclusion of energy dissipation, the better agreement is obtained. The nonlinear effects are more shown in measured data of case 1 while the dissipation effects are relatively small. Further experiments are in progress to verify the present method more clearly.

Table 1. Input data of physical experiment

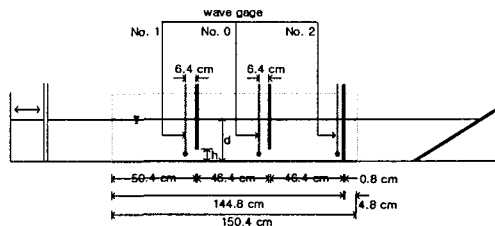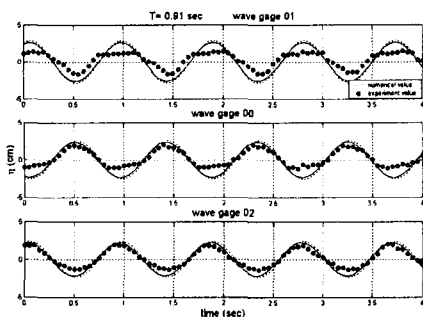|	period	Hi	h/d	r	e
case1	0.91	3.2cm	0.75	0.125	0.100
case2	0.7	2.7cm	0.75	0.290	0.215

Fig. 5. Physical layout of experiment.

Fig. 6. Comparison with measured wave profile for period 0.91sec (solid line: with losses, dashed line: without losses).
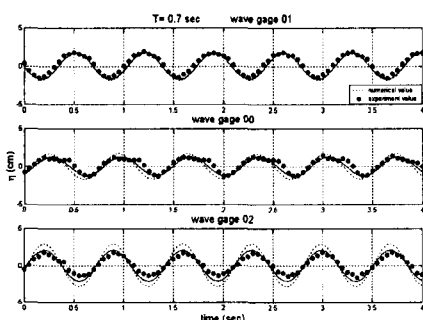

Fig. 7. Comparison with measured wave profile for period 0.7sec (solid line: with losses, dashed line: without losses).

6. Conclusion

The present paper presents a method to take into account the effects of energy losses due to vortex shedding from the lower edges of surface-piercing vertical plates. Stiassnie (1984)'s formula was used in estimating the energy dissipation coefficients due to a vortex motion in a single barrier. The numerical model employed here is an extended mild-slope equation which has been proposed by Lee and Lee (2001) and Lee and Lee (2003) using a plane wave method without inclusion of evanescent modes. The scattering term, which generates the scattering waves, is determined by the gradient of surface velocity potential across the barrier. Evanescent modes are only considered in predicting the reflection ratio against the vertical barrier.

The numerical results are compared with experimental

data carried out in the wave flume. The agreement is generally satisfactory with the inclusion of energy dissipation effects and indicates that the present method is able to adequately account for the arbitrary energy dissipation.

References

Berkhoff, J.C.W., 1972. Computation of combined refraction diffraction. *Proc. 13th Conf. Coastal Eng.*, pp. 471-490.

Copeland, G.J.M., 1985. A practical alternative to the mild slope wave equation. *Coastal Engineering* 9, pp. 125-149.

Lee, J.L., 1998. Boundary treatment in a hyperbolic wave model. *J. the Korean Society of Civil Engineers* 18(II-6), pp.601-612.

Lee, J.L., and Lee, D.Y., 2003. Modeling of wave scattering by vertical barriers. The *Proc. of 13th International Offshore and Polar Engineering Conference*, ISOPE, Vol. 3, pp. 773-780.

Lee, J.L., and Lee, K.J., 2001. Effect of a surface-piercing vertical thin breakwater to harbor tranquility. *The First Asian and Pacific Coastal Engineering Conference*, pp. 186-195.

Madsen, P.A., and Larsen, J., 1987. An efficient finite-difference approach to the mild-slope equation. *Coastal Engineering* 11, pp. 329-351.

Mei, C.C., 1983. *The Applied Dynamics of Ocean Surface Waves*. Wiley, New York.

Ohyama, T. and Tsuchida, M., 1997. Expanded mild-slope equations for the analysis of wave-induced ship motion in a harbor. *Coastal Engineering* 30, pp. 77-103.

Sawaragi, T., Aoki, S., and Hamamoto, S., 1989. Analysis of hydrodynamic forces due to waves acting on a ship in a harbor of arbitrary geometry. *Proc. 8th Int. Conf. Offshore Mech. and Arctic Eng.*, ASME, pp. 117-123.

Smith, R., and Sprinks, T., 1975. Scattering of surface waves by a conical islands. *J. Fluid Mech.* 72, pp. 373-384.

Stiassnie, M., Naheer, E., and Boguslavsky, I., 1984. Energy losses due to vortex shedding from the lower edge of a vertical plate attacked by surface waves. *Proc. R. Soc. Lond.* A396, pp.

131-142.

Ursell, F., 1947. The effect of a fixed vertical barrier on surface waves in deep water. *Proc. Camb. Phil. Soc.* 43, pp. 347-382.